RAPID COMMUNICATIONS

PHYSICAL REVIEW B VOLUME 43, NUMBER 1 1 JANUARY 1991

Non-Rayleigh statistics of waves in random systems

N. Shnerb and M. Kaveh
Department of Physics, Bar-Ilan University, Ramat-Gan, Israel
(Received 16 July 1990)

We show that, when the effective disorder of a system increases, non-Rayleigh statistics characterize the intensity fluctuations of a propagating wave in a random medium. We find a single scaling parameter that describes the intensity distribution function, which depends on the conductance and transmission coefficient of the system. Our analytical results are in agreement with the results of numerical simulations, which indicates that the statistics of transmitted waves and reflected waves in restricted geometries is very different.

One of the fundamental properties related to the propagation of waves in disordered systems is their random amplitude fluctuations which obey the Rayleigh law of Gaussian statistics. This general result holds for the wave function of quantum waves as well as for classical electromagnetic waves[1-4] or acoustical waves. The inhomogeneities of the system induce strong multiple scattering of the wave which leads to large local intensity fluctuations at any given point. The basic Rayleigh law derives from the central-limit theorem in which the amplitude of the wave can be decomposed into a sum of random, statistically independent amplitudes created by different Feynman multiply scattered trajectories. Are there conditions under which one can obtain the breakdown of Rayleigh statistics? This is of recent experimental interest, where it was observed[5] that when the disorder increases, non-Rayleigh statistics appear.

In this paper, we derive the conditions for non-Rayleigh statistics and show that the statistical properties of the intensity of a wave at any given point in the system is determined by a single scaling parameter. For transmitted waves, this parameter S_t is the crossing probability between any two Feynman trajectories which depend on the conductance g and the transmission coefficient T of the system. When gT^2 decreases, the intensity fluctuations obey non-Rayleigh statistics. For reflected waves, the relevant parameter S_r is different and depends on $(\lambda/l)^{d-1}$, where l is the elastic-transport mean free path and d is the dimensionality of the system.

Our analytical results for the non-Rayleigh distribution functions for the intensity of transmitted or reflected waves are in agreement with our numerical simulations.

We first present our main results for non-Rayleigh statistics in terms of the moments of the intensity. For Rayleigh statistics, $\langle I^n\rangle/\langle I\rangle^n = n!$. By contrast we find

$$\langle I^n\rangle/\langle I\rangle^n = n!f(n)\,, \tag{1}$$

where $f(n)$ is due to interference effects which we discuss below. The interesting result is that $f(n)$ is different for transmitted and reflected waves. It is an increasing function for transmitted waves and a decreasing function for reflected waves. For transmitted waves and small values of S_t, we get

$$f_T(n,S_t) = 1 + \tfrac{1}{2}S_t(n^2-n)\,, \tag{2}$$

where S_t represents the crossing probability of two Feynman trajectories which we calculate later.

For reflected waves we obtain

$$f_R(n,S_r) = (1-S_r)^n L_n[S_r/(1-S_r)]\,, \tag{3}$$

where S_r is the probability to return to the same channel (which is derived below) and $L_n(x)$ are the Laguerre polynomials. The function $f_R(n,S_r)$ is always smaller than unity.

We have performed numerical simulations to study the intensity statistics by using the method of Edrei, Kaveh, and Shapiro.[6] In Fig. 1(a), we plot $f_T(n,S_t)$ and in Fig. 1(b) we plot $f_R(n,S_r)$ for a sample of length $L=50$ and width $W=7$. The solid curves correspond to Eqs. (2) and (3) and the squares represent the numerical simulations. The agreement is evident from the figures. It should be noted that the deviations from Rayleigh statistics for transmitted waves are opposite to those for reflected waves, as will be explained later. From the intensity moments, we derive all the distribution functions by using the Fourier-transform method. For transmitted waves, we obtain the following analytical result:

$$P_T(I,S_t) = \langle I\rangle^{-1}\exp(-I/\langle I\rangle)\{1+\tfrac{1}{2}S_t[(I/\langle I\rangle)^2 - 4I/\langle I\rangle + 2]\}\,. \tag{4}$$

In Fig. 2, we plot $P_T(I,S_t)$. The squares correspond to the numerical simulations and the solid curve represents Eq. (4). The agreement is very good. For comparison, we plot (dashed curve) the negative-exponential distribution function $\langle I\rangle^{-1}\exp(-I/\langle I\rangle)$, which decreases much more slowly than the numerical results.

We now present the underlying ideas upon which the distribution functions are based. The Rayleigh distribution function is obtained by assuming that all the different Feynman trajectories which represent the partially multiply scattered waves are independent in the sense that they acquire a different independent random phase for each path. The amplitude of the wave at a given point in the system is given by

$$E = \sum_\alpha E_\alpha\,, \tag{5}$$

where we sum over all Feynman trajectories. The aver-

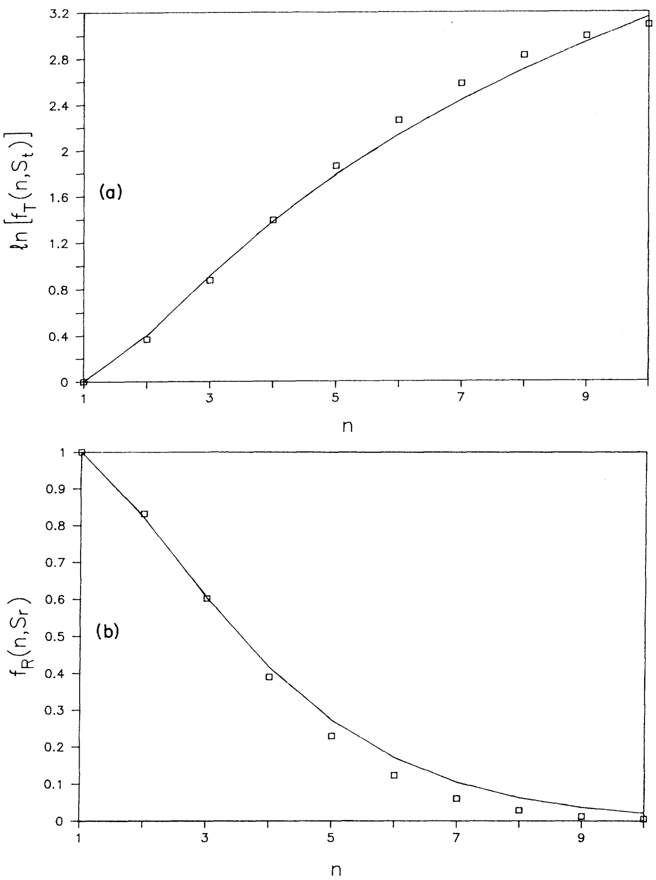

FIG. 1. (a) $\ln f_T(n,S_t)$ as a function of n. The squares represent the numerical simulations and the solid curve Eq. (2). (b) $f_R(n,S_r)$ as a function of n. The squares represent the numerical simulations and the solid curve Eq. (3).

aged nth moment of the intensity is given by

$$\langle I^n\rangle = \sum_{\substack{\alpha_1\cdots\alpha_n\\ \beta_1\cdots\beta_n}} \langle E_{\alpha_1}\cdots E_{\alpha_n}E^*_{\beta_1}\cdots E^*_{\beta_n}\rangle . \qquad (6)$$

When all the Feynman trajectories are assumed to be independent, it follows that

$$\langle E_\alpha E^*_\beta\rangle = \delta_{\alpha,\beta}\langle I\rangle \qquad (7)$$

and the nonzero contributions in (6) arise only from pairs $\langle E_\alpha E^*_\beta\rangle$ when $\alpha=\beta$. Since there are $n!$ such possible pairs, we obtain $\langle I^n\rangle = n!\langle I\rangle^n$. The origin of non-Rayleigh statistics is due to the intersections between Feynman trajectories. Consider two Feynman trajectories which intersect, as shown in Fig. 3. We label these two trajectories with four indexes: (i,j) to represent the trajectories before they intersect and (I,J) to represent the trajectories after they intersect. We then have *four* trajectories which interfere and lead to an amplitude

$$E = E_{iI}+E_{iJ}+E_{jI}+E_{jJ} . \qquad (8)$$

Consider for example, the averaged second moment $\langle I^2\rangle$ which will include two terms of the form $\langle E_{iI}E^*_{iJ}E_{jI}E^*_{jJ}\rangle \propto \langle E^{i\Delta\phi}\rangle$, where $\Delta\phi$ is the phase difference

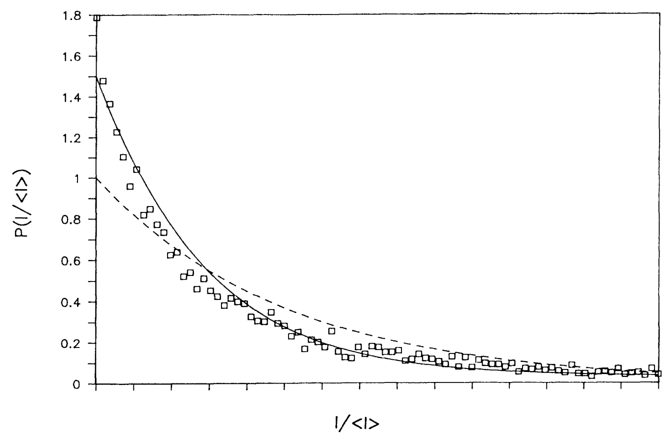

FIG. 2. $P(I/\langle I\rangle)$ as a function of I for transmitted waves. The squares represent the simulations and the solid curve Eq. (4). The dashed curve corresponds to the Rayleigh statistics.

between the four trajectories (see Fig. 3) and is given by $\Delta\phi = (\phi_i+\phi_I)-(\phi_i+\phi_J)-(\phi_j+\phi_I)+(\phi_j+\phi_J)$. Since each part of the trajectory appears *twice* and each time with a phase with *opposite* sign, it follows that $\Delta\phi=0$. This enhances the second moment and consequently all the higher moments. We denote the crossing probability of two trajectories in Fig. 3 by S_t. The second moment is given by

$$\langle I^2\rangle = 2\langle I\rangle^2 + 2S_t\langle I\rangle^2 . \qquad (9)$$

The first (Rayleigh) contribution arises from pairing of two trajectories and the second term results from the interference caused by four trajectories that were created by two intersecting trajectories. We now calculate all the possible nonzero terms which arise in the nth moment $\langle I^n\rangle$ in Eq. (6) due to the crossing of two trajectories. The number of possible terms of the form $\langle E_{\alpha L}E_{\alpha K}E^*_{\beta L}E^*_{\beta K}\rangle$ is $\binom{n}{2}^2$. From *each* set of amplitudes $E_{\alpha_1}\cdots E_{\alpha_n}$ and $E^*_{\beta_1}\cdots E^*_{\beta_n}$, the number of possible remaining pairs $\langle E^*_{\alpha_m}E_{\beta_M}\rangle$ is $(n-2)!$. Thus, the number of nonzero terms resulting from the ensemble average of Eq. (6) is $2\binom{n}{2}^2(n-2)!$. Since the crossing probability is S_t, the contribution to the nth moment is $2\binom{n}{2}^2(n-2)!S_t\langle I\rangle^n$ and

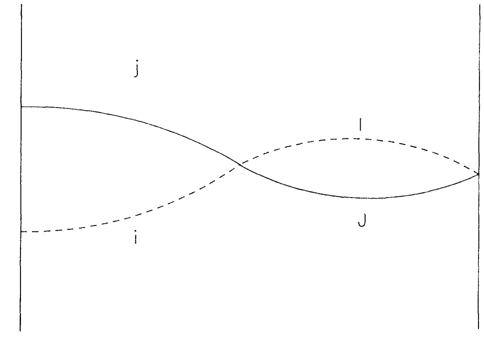

FIG. 3. Typical two-crossing Feynman trajectories for transmitted waves.

the entire nth moment is given by

$$\langle I^n \rangle = n!\langle I \rangle^n + 2\binom{n}{2}^2 (n-2)! S_t \langle I \rangle^n . \tag{10}$$

From (10), we obtain $f_T(n,S_t)$, as given in Eq. (2). We conclude that the crossing of two Feynman trajectories dramatically enhances $\langle I^n \rangle$.

We now derive the scaling dependence of the crossing probability S_t and show that it depends on the conductance and on the transmission coefficient of the system. A Feynman trajectory in a d-dimensional system occupies a volume $(\lambda^{d-1} l)(L/l)^2$. The volume fraction of a Feynman trajectory for $W<L$ is therefore $(\lambda/W)^{d-1}(L/l)$ and is equal to g^{-1}. The probability that two typical Feynman trajectories will cross at a given point is therefore g^{-2}. The effective number of points available for a random-walk trajectory is $N=W^{d-1}L/\lambda^{d-1}l$ which is equal to g/T^2. From this result, the crossing probability for $W<L$ may be written as

$$S_t = 1-(1-g^{-2})^{g/T^2}; \quad g \geq 1 . \tag{11}$$

We see that as $g \rightarrow 1$, $S_t \rightarrow 1$ and we reach the strong-disorder limit in which localization sets in. Here, we are interested in the weak-disorder limit in which $g \gg 1$ and the propagation of the wave in the medium is diffusive. In this limit, S_t may be expanded to give

$$S_t = 1/gT^2 . \tag{12}$$

In this regime, the transmission coefficient $T \ll 1$ and the conductance $g \gg 1$. We confine ourselves to $gT^2 > 1$, which corresponds to small values of S_t. In general, $P_T(I,S_t)$ is a function of only one scaling parameter S_t which is given by (11).

Our expression for $P_T(I,S_t)$ in Eq. (4) is valid only for $S_t \ll 1$ for which multiply-crossing Feynman trajectories can be neglected. When S_t increases, one should also consider all higher-order crossing effects. In this case, the calculation of $P_T(I,S_t)$ for $S_t \rightarrow 1$ is an extremely complex problem, since it must include multiple-crossing Feynman trajectories.

We now turn to the statistical properties of reflected waves and show that they differ greatly from those of transmitted waves. We first show that, in contrast to transmitted waves, the crossing of two Feynman trajectories for reflected waves has only a negligible effect on the intensity statistics. There are two possible crossing effects for reflecting waves which are shown in Fig. 4. Figure 4(a) represents crossing between two different Feynman trajectories, whereas Fig. 4(b) represents a self-crossing of a single trajectory.

The averaged length of a reflecting trajectory is Pl where we find that $P \simeq 5$–6. For the case presented in Fig. 4(a), the crossing probability is $(\lambda/W)^{d-1}P$ which is extremely small for $W \gg \lambda$ and does not affect the intensity statistics. Similarly, we find that the self-crossing probability [Fig. 4(b)] for $Pl < W$ is given by $(\lambda/l)^{d-1}/P^{d-2}$. In the weak-disorder limit, where $l \gg \lambda$, this self-crossing will affect intensity statistics only slightly. We therefore conclude that the mechanism of Feynman trajectory crossing, which is crucial for the non-Rayleigh statistics for transmitted waves, is not important for the statistics of

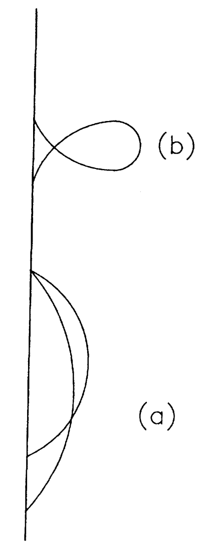

FIG. 4. (a) Typical two-crossing Feynman trajectories for reflected waves. (b) Typical self-crossing Feynman trajectory for reflected waves.

reflected waves because the trajectories are too small. However, the statistics of the reflected wave will change dramatically if the number of input channels is reduced. This is of general interest since this was recently achieved experimentally[4,7] in the study of long-range correlations.[8-10] Denoting $r_{\alpha\beta}$ as the reflection amplitude from channel α to channel β, we can express the second intensity moment by

$$\langle I^2 \rangle = \sum_{\substack{\alpha,\alpha' \\ \gamma,\gamma'}} \langle r_{\alpha\beta} r^*_{\alpha'\beta} r_{\gamma\beta} r^*_{\gamma'\beta} \rangle . \tag{13}$$

Introducing $x \equiv \sum_{\alpha \neq \beta} |r_{\alpha\beta}|^2$ and $y \equiv |r_{\beta\beta}|^2$ we get

$$\langle I^2 \rangle = (2x^2 + 2xy + y^2) \tag{14}$$

and for the nth moment,

$$\langle I^n \rangle = \sum \binom{n}{m} (n-m)! x^{n-m} y^m . \tag{15}$$

From Eq. (15), we get

$$\langle I^n \rangle / \langle I \rangle^n = n!(1-S_r)^n L_n [S_r/(1-S_r)] ,$$

where $y \equiv S_r$ is the probability to return to the *same* channel, which is given by $4(\lambda/lP)^{d-1}$. This defines the function $f_R(n,S_r)$ in Eq. (3). From the numerical simulations, we have found $S_r = 0.6$, from which we see from Fig. 1 that strong deviations are found from Rayleigh statistics.

Finally, we consider the role of absorption on non-Rayleigh statistics. There are two different regimes $L_a > L$ and $L_a < L$. For $L_a > L$, we find that stronger absorption reduces the non-Rayleigh statistics for transmitted waves and enhances them for reflected waves. The effect of absorption is important for reflected waves only when the absorption length L_a is smaller than the averaged reflected trajectory lP. In this case, S_r is changed to

$(\lambda/L_a)^{d-1}$ and increases as L_a is shorter. On the other hand, absorption cuts the Feynman trajectories for transmitted waves and therefore reduces the crossing probability, which becomes $S_t = \lambda^{d-1} L_a^{3-d}/Ll$. Thus, reducing L_a causes the intensity statistics to be more Rayleigh-like. This is so only for $L_a > L$. For $L_a < L$, the crossing probability increases, and in the limit $L_a \ll L$, the dominant contribution to the intensity comes from ballistic trajectories which contribute a nonfluctuating part to the intensity and to a peak in the distribution $P_T(I)$. Such behavior was recently observed by Garcia and Genack[5] for samples with $L_a \simeq \frac{1}{6} L$ where $P_T(I)$ was found to undergo a maximum followed by a stretched exponential. A detailed comparison between the experiment of Garcia and Genack[5] and $P_T(I)$ for $L_a \ll L$ will be presented elsewhere.

The non-Rayleigh behavior in this limit is due to the fact that the number of possible trajectories N decreases appreciably and do not allow the use of the central-limit theorem (which holds when $N \to \infty$).

In summary, we have calculated the non-Rayleigh statistics for transmitted and reflected waves of disordered systems. They are shown to depend only on a single parameter which for transmitted waves is the crossing probability of two Feynman trajectories and, for reflected waves, the probability for returning to the same channel. Our calculated distribution functions are in agreement with the results of numerical simulations.

[1] A. Ishimaru, *Wave Propagation and Scattering in Random Media: Multiple Scattering Turbulence, Rough Surfaces and Remote Sensing Vol. 2* (Academic, New York, 1978).
[2] V. I. Tatarskii and V. U. Zavortnyi, in *Strong Fluctuations in Light Propagation in Randomly Inhomogeneous Medium,* edited by E. Wolf [Prog. Opt. **18**, 204 (1980)].
[3] J. W. Goodman, J. Opt. Soc. Am. **66**, 1145 (1976); J. W. Goodman, *Statistical Optics* (Wiley, New York, 1985).
[4] B. Shapiro, Phys. Rev. Lett. **57**, 2168 (1986).
[5] N. Garcia and A. Z. Genack, Phys. Rev. Lett. **63**, 1678 (1989).
[6] I. Edrei, M. Kaveh, and B. Shapiro, Phys. Rev. Lett. **62**, 2120 (1989).
[7] M. P. van Albada, J. F. de Boer, and A. Lagendijk, Phys. Rev. Lett. **64**, 2787 (1990).
[8] M. J. Stephen and G. Cwilich, Phys. Rev. Lett. **59**, 285 (1988).
[9] Shechao Feng, Charles Kane, Patrick A. Lee, and A. Douglas Stone, Phys. Rev. Lett. **61**, 834 (1988).
[10] S. Pnini and B. Shapiro, Phys. Rev. B **39**, 6986 (1989).